PNC-TN9410 86-034

Presented at the 2nd International Topical
Meeting on Power Plant Thermal Hydraulics
and Operations

CHARACTERISTICS OF NATURAL CIRCULATION IN THE ATR PLANT

HIROYASU MOCHIZUKI
KIMINORI SHIBA

March, 1986

OARAI ENGINEERING CENTER
POWER REACTOR AND NUCLEAR FUEL DEVELOPMENT CORPORATION

動力炉・核燃料開発事業団（Power Reactor and Nuclear Fuel Development Corporation）

PNC-TN9410 86-034

March, 1986

CHARACTERISTICS OF NATURAL CIRCULATION IN THE ATR PLANT

H. Mochizuki* and K. Shiba*

ABSTRACT

Coolability of natural circulation under the condition of lowered reactor water levels has been studied on a recirculation system of a pressure-tube-type heavy water reactor ATR (Advanced Thermal Reactor) to be developed in Japan. Onset boundary of flow instability induced in natural circulation was also found out experimentally. Natural circulation flow rate was predicted by a code based on a slip model within an accuracy of about 15%. The code was also successfully applied to analysis of flow oscillation excited in low heating power region.

---

* ATR Safety Section, Safety Engineering Division, O-arai Engineering Center, PNC.

INTRODUCTION

Advanced thermal reactor (ATR) is a heavy-water moderated light-water cooled pressure-tube type reactor, which is equipped with a recirculation system as shown in Fig. 1. After being fed with recirculation pumps to a water drum coupled with check valves, subcooled water is distributed to each pressure tube through inlet pipes, and turns into two-phase mixture in a core. Two-phase mixture flows into a steam drum via outlet pipes, and is separated into steam and saturated water with steam separators installed within the steam drum. Steam is supplied to turbines, and returns to the steam drum through a feed water system. Saturated water and feed water is mixed into subcooled feed water, which is fed back via downcomers to the water drum.

The core is ordinarily cooled by this forced circulation. In an emergency case when any important component gets out of order or any abnormal transient takes place, however, the reactor is shutdown, and shifts from the forced circulation mode to a nutural circulation mode. In this case, water level in the steam drum significantly lowers, because the recirculation system has a comparatively small coolant inventory, and main steam escaping from the system is usually more than the supply of feed water. Further, in another emergency case of abnormal transient where system pressure rises, water level also tends to lower owing to collapsing of steam voids in the core.

The ATR demonstration plant is designed so that water level might not go down below the bottom of the steam drum in these cases. If water level would appear within the downcomer in a rare incident unable to be anticipated, however, it may easily lower to the upper end of the core because

of small coolant inventory in the downcomer. Therefore it is necessary to investigate whether the core can be cooled under such conditions or not.

Nakajima[1] has so far reported that the ATR core can be cooled well by natural circulation formed under the condition of nearly atmospheric pressure and lowered water level, and of high pressure (about 7 MPa) and high water level. However, it is necessary for the actual plant to confirm that the core can be also cooled well by natural circulation formed under the conditions of high pressure and lowered water level. Thus taking account of the actual plant operation condition, we have made tests under the conditions where subcooling of coolant and water level are extensively changed. Further we compare measured natural circulation flow rate with predictions by a code based on the slip model.

Flow oscillation somewhat unfavourable for core cooling is likely to be excited in natural circulation of systems, which are provided with long horizontal parallel outlet pipes. Then instability boundary of the ATR recirculation system has been studied at near atmospheric pressure by Fukuda[2], using the Heat Transfer Loop(HTL). However, little is known on instability boundary under the condition where system pressure is comparatively high just after reactor scram; hence, we have also carried out experiments to find out the instability boundary at high pressure and instability pattern excited.

TEST APPARATUS AND TEST CONDITIONS

Test Apparatus

HTL was used in the natural circulation tests. The loop nearly

simulates the actual 2 channels of the recirculation system of the ATR plant shown in Fig. 1.

Figure 2 shows a flow diagram of HTL, which is provided with the same pressure tubes (inner diameter: 117.8 mm, length: about 5 m) and outlet pipes (inner diameter: 73.9 mm, length: about 25 m) with inner diameter and length as those used in the actual plant, in order to remove the scale effects on two-phase flow from measured results. On the other hand, the piping from the steam drum to inlet of the heating section is different in dimension from that of the actual plant. Therefore, pressure loss in this piping including bends and check valves was made equal to that expected in the actual plant, by adjusting the opening of valve-V1 and valve-V3. Hence, relation between pressure drop and flow rate in the inlet section of the actual plant is non-linear as shown in Fig. 3, since check valves are put in this section. Therefore, the opening of the valve-V3 was adjusted so that pressure loss might be exactly same only at 2 t/h of flow rate between HTL and the actual plant.

In the heating section, 28- or 36-rod bundles were put. Their cross sections are shown in Fig. 4. The 28-rod bundle heaters have the same size as fuel assemblies used in the prototype reactor Fugen, and the 36-rod bundle heaters are the same in size as fuel assemblies of the ATR demonstration plant. The effective heated length of these heaters is 3.7 m. The heater rods are tied with the same spacers as those of the actual fuel. Consequently, pressure loss in the heating section where two-phase mixture flows, is exactly the same as in the core of the actual plant. Each heater rod bundle is heated using a power supply of 7 MW at maximum, by the direct electrification method. They were provided with thermocouples upstream of spacers. Table 1 shows comparison between the test apparatus and the

recirculation system of the prototype reactor or the demonstration plant of the ATR.

The circulation flow rate of the entire test loop is measured within error of 1% with a turbine flow meter installed upstream of the pre-heater. On the other hand, in order to accurately measure even low flow rate including reverse flow, ultrasonic flow meters available at high temperature were pressed with clamp onto inlet pipes of each channel. Error of the ultrasonic flow meter was estimated to be within 3% from the weight calibration. Needletype densitometers were provided at the entrance and exit of the outlet pipes. The water level from the lowest end of the downcomer to water surface in the steam drum was measured by a differential pressure transducer. Readings were corrected to condition of no difference in liquid density between the downcomer and a conduit. Error in measured water level was estimated to be within 3%.

Steam generated in the heating section was condensed to water in a condenser and stored in the steam drum-I. Water in this drum is carried by a pump to the steam drum-II to maintain the water level in the steam drum-II or downcomer at a fixed level.

Test Conditions

Two types of tests were conducted: steady tests where thermal hydraulic parameters like system pressure, heating power, and subcooling are kept as constant as possible, and transient tests where heating power varies in the same way as decay heat does. The test conditions are tabulated in Table 1. In the steady tests, water level in the downcomer was changed in the range of -2 to 10.1 m (the water level is measured from the upper end of the heater rod bundle). The conditions of the steady tests were decided so

as to comprehend operational conditions after reactor shutdown of the ATR plants.

Since the transient tests were carried out under the condition where heating power varies, effect of time-dependent heating power on flow characteristics is found out from comparison of measured results between the steady and the transient tests. Generally, opening of the check valve reduces as flow rate decreases, resulting in increase in flow resistance of the system. In order to simulate such a condition, the tests were conducted by closing the manually operated valve-V3 installed downstream of the pre-heater. The flow resistance in the system was varied in the range of 30 to 3000 in terms of the pressure loss coefficient.

ANALYTICAL MODEL

A code named ACCEPT-II was developed to analyze transient flow including oscillation frequently observed in the system having parallel channels.

Basic Equations

According to flow conditions, the loop shown in Fig. 1 can be divided into three sections: a single-phase flow section, a two-phase flow section and the drum. Flow in the single-phase flow section is analyzed by a piston flow model, the flow in the two-phase flow section by a slip model, and the drum by a model considering only the mass and energy balance.

The following correlations were applied to calculate pressure loss for single-phase flow.

Straight pipes: Blasius's[3] or Nikuradse's[4] formula:

$$\left.\begin{aligned} \lambda &= 0.3164\ Re^{-0.25} \qquad 2300 \leqq Re \leqq 10^5 \\ \lambda &= 0.0032 + 0.221\ Re^{-0.237} \qquad 10^5 < Re < 10^8 \end{aligned}\right\} \quad (1)$$

Bends: Weisbach's formula:

$$\zeta_b = 0.131 + 0.1632\ (D/R)^{3.5} \quad (2)$$

Changed shapes:

Gibson's results[5] (sudden expansion).

Richer's results[6] (sudden reduction).

Spacer: Empirical formula:

$$\left.\begin{aligned} \zeta_{sp} &= 2.7 - 1.55\ (\log Re - 4) \qquad Re \leqq 8 \times 10^4 \\ \zeta_{sp} &= 1.3 \qquad\qquad\qquad\qquad Re > 8 \times 10^4 \end{aligned}\right\} \quad (3)$$

Valve: Measured values.

In the analysis of the two-phase flow section, the following void-quality correlation was employed;

$$\alpha = \beta^3 = \left[\ 1 + \frac{\rho_g\ (1 - x)}{\rho_l\ x}\ \right]^{-3} \quad (4)$$

This correlation was developed on the basis of measurements in natural circulation in the HTL loop.

This relation between void and quality measured in the natural circulation test system, gives lower void fraction than the modified Bankoff expression proposed by Jones[7], as shown in Fig. 5. Since voids in the core play important role of driving force of coolant in the natural circulation condition, choice of the correlation has an influence

on prediction accuracy in flow rate. Therefore, the correlation measured in HTL was used in the code. The pressure loss for two-phase flow was estimated, by multiplying values evaluated by the Eqs. (1) to (3) by two-phase flow multipliers measured by Sugawara[8].

The flow rate distribution in multichannels is calculated under conditions that pressure loss from the water drum to the steam drum is equal among the channels, and that the pressure loss in the route starting at the steam drum, going through the water drum and the test sections, and coming back to the steam drum is zero.

The pressure loss in the section from steam drum to water drum is estimated from pipe frictional loss, head and acceleration loss by

$$P_W - P_D = a_d \frac{dw_d}{dt} + b_d \ . \tag{5}$$

The pressure loss in a given channel existing between the water drum and the steam drum is estimated as below.

$$P_D - P_W = a_i \frac{dw_i}{dt} + b_i \qquad (i=1,\ldots,N) \tag{6}$$

Since mass should totally balance in the system, the following equation is derived.

$$\sum_{i=1}^{N} A_i w_i = A_d w_d \tag{7}$$

By use of the Eqs. (5), (6) and (7), the flow rate in each channel must be decided so as to satisfy the following system of equations:

$$a_i \frac{dw_i}{dt} + \frac{a_d}{A_d} \sum_{i=1}^{N} A_i \frac{dw_i}{dt} + b_i + b_d = 0 \ . \qquad (i=1,\ldots,N) \tag{8}$$

This system of equations can be also expressed by the matrix:

$$\begin{pmatrix} a_1+K_1 & K_2 & \cdots & K_N \\ K_1 & a_2+K_2 & \cdots & K_N \\ \cdot & & & \cdot \\ \cdot & & & \cdot \\ K_1 & \cdots & K_{N-1} & a_N+K_N \end{pmatrix} \begin{pmatrix} \dot{w}_1 \\ \dot{w}_2 \\ \cdot \\ \cdot \\ \dot{w}_N \end{pmatrix} = \begin{pmatrix} -b_1-b_d \\ -b_2-b_d \\ \\ \\ -b_N-b_d \end{pmatrix} \qquad (9)$$

where K_i is the constant determined for each channel by

$$K_i = \frac{A_i}{A_d} a_d \qquad (i=1,\ldots,N) \ . \qquad (10)$$

Time derivatives of flow rate $\dot{w}_i$ are obtained by solving the matrix of Eq. (9), and then the flow rate w_i is determined from $\dot{w}_i$ by integration.

RESULTS AND DISCUSSION

Figure 6 shows dependence of flow rate in natural circulation on heating power. This dependence was measured in the range of the downcomer water level from 1 to 10.1 m at 6 MPa of system pressure and 10±0.5 °C of subcooling. The closed symbols are the results on the 28-rod bundle, and open symbols are the results on the 36-rod bundle. As is seen in Fig. 6, natural circulation flow rate increases with increasing of heating power, or with rising of water level. The channel power given in Fig. 6 corresponds to linear heat rate ranging from 13.5 to 108 KW/m. In either case, the heater surface temperature did not change at all.

However Fig. 6 shows that the flow rate tends to level off as heating power increases, which brings about problems of coolability in high heating power. The dotted lines in Fig. 6 show the results by the code ACCEPT-II for the system incorporating with the 36-rod bundle.

The analytical dependence of natural circulation flow rate upon water level generally agrees with experimental one; however, slight disagreement is recognized in the case where water level is 3 m or below and heating power lowers to 200 KW or less. This may be attributed to poor accuracy in flow rate measured with the turbine flow meter, besides reducing accuracy in prediction by the code, since the disagreement appears in low flow rate of 1.5 t/h or less.

Figure 7 shows the channel flow rate measured at 145 KW of heating power in the system incorporating with the 28-rod bundle as a function of inlet subcooling. Increase in subcooling is more effective to suppression of boiling in the heating section than to increase in coolant density, which results in reducing driving force, and eventually in diminishing flow rate. The test has reproduced such process well. However the heater surface temperature did not change and cooling was favorably accomplished even under this condition. Solid lines in Fig. 7, which show the analytical results by the code ACCEPT-II, agree with the measured results within about 30%. The comparison between the measured and calculated channel flow rates illustrated in Fig. 8 shows that the code ACCEPT-II predicts natural circulation flow rate within an accuracy of about ±15%.

Figure 9 shows results of the transient test conducted under the condition where bundle power varies accordingly to the ANS standard decay power equation[9] from the initial power of 200 KW, which is equivalent with the power at 60 s after reactor scram from the power of 5 MW. The reason why 60 s after reactor scram is selected is that earlier than 60 s, the recirculation pump is still in the course of coast-down and no pure natural circulation appears yet. From this figure, we can see that flow rate decreases with reduction of the heating power. Figure 10 displays flow

rate and heating power sampled at an interval of 30 seconds, together with the solid line showing results of the steady test. As is seen in Fig. 10, the transient test results are practically equal to those of the steady test. This suggest that change in heating power influences flow rate instantaneously and no non-steady effects are brought about into flow characteristics.

It has been concluded from the present tests that the heater bundle can be favorably cooled provided that the heating power is at the level of decay heat and water level in the downcomer is higher by more than 1 m than the upper end of heated portion of the bundle. Next, to find out how much the water level could be lowered without deteriorating coolability, a test was performed at 150 KW of heating power and about 10 °C of inlet subcooling, by lowering the downcomer water level gradually from the upper end of the heater. As shown in Fig. 11, the test reveals that when the downcomer water level drops by about 1.5 m from the upper end of the heater, the heating section dryouts and its surface temperature rises suddenly. In this case, void fraction at the outlets of the heating sections indicates that water is expelled from the upper portion of the heating section at the time sufficiently before dryout occures. This implies that boiling surface appears in the upper portion of the heating section under this situation, and flow rate should be equal to evaporation rate from this boiling surface.

Flow oscillation in natural circulation is excited under the condition where the heating power is reduced below the lower boundary or exceeded beyond the upper boundary. Figure 12 shows boundaries measured at 10.5 m of water level. The upper boundary increases with increasing of pressure. On the other hand, the lower boundary is less dependent on pressure than the upper boundary.

Figure 13 shows flow oscillation excited at 100 KW of heating power per channel, 10 °C of inlet subcooling, and 6.1 MPa of the system pressure. The upper figure illustrates the measuring result, and the lower, the result by the code ACCEPT-II. Flow rates in two channels lag from each other by 180 °C. The experimental period is 7 seconds, while the code predicts 8.1 seconds about 15%-longer than the experimental one. The experimental amplitude is 2.6 t/h, which is about 50% smaller than the predicted one. It is concluded from Fig. 13 that the code predicts flow oscillation well in the whole.

In order to determine a pattern of flow oscillation excited below the lower boundary in natural circulation of the ATR plants, characteristics of flow oscillation was investigated by changing opening of the valve-V3 installed at the inlet section of the parallel two channels (see Fig. 2). As is seen in Fig. 14, observed amplitude of flow rate gradually increases as the opening of the valve-V3 decreases from 15 to 5%. Void fraction at the entrance and exit of outlet pipes fluctuates irregularly when flow rate oscillates with small amplitude; however, void fraction only at the exit fluctuates synchronously with movement of flow rate when it oscillates with large amlitude. This fact suggests that flow regime is not uniform throughout the outlet pipes in the case of flow oscillation with large amplitude; i.e. bubbly flow near the heated section and slug flow far away from the heated section.

In order to confirm this infer, transformation of flow regimes was observed in a full-scale lucite mock-up simulating the outlet pipes of the ATR plant. Observation revealed that air bubble flow at the entrance near the heating section turns into stratified flow at the middle of horizontal section, and ultimately into slug flow at vertical section in front of the

steam drum.

In order to find out how pressure loss in the inlet section affects flow oscillation, measured ratios of amplitude to average flow rate are plotted in Fig. 15 against pressure loss coefficient of the valve. Figure 15 shows that the ratio increases with increasing of loss coefficient, and it exceeds unity at the loss coefficient of 10^3 or more, which means that flow rate swings back to a reverse-flow region. These facts suggests that flow oscillation exceed below the lower boundary in the ATR system is somewhat different from density wave oscillation although wave form illustrated in Fig. 14 is similar to that of density wave, and is categorized into flow-regime-induced oscillation.

At present it is difficult to forecast the flow oscillation shown in Fig. 14 by the code ACCEPT-II, since the code assumes the flow within pipes to be uniform two-phase flow. In future, it is therefore necessary to incorporate a model of the pressure loss dependent on the pattern of two-phase flow in the code.

In the power region below the lower boundary, no temperature change on the heater surface was observed at all even if the flow oscillation induced reverse flow. Therefore the flow oscillations below the lower boundary is not an important issue for cooling of fuel bundles. In the case when heater power exceeds the upper boundary, on the other hand, heater surface would repeat dryout and rewetting syncronously with oscillation of flow rate, or be burn-out. In natural circulation in the actual plant, consequently, power of fuel rod bundle should be surpressed under the upper boundary, to prevent this situation.

CONCLUSIONS

The following conclusions were obtained from the natural circulation tests conducted in the recirculating system simulating the ATR plants.

(1) Flow rate in natural circulation increases with increasing of heating power, decreasing of subcooling, and rising of water level.

(2) Heater rod bundles with power equivalent with decay heat do not dryout until water level drops from the upper end of the heater by about 1.5 m or more.

(3) Flow oscillation with a long period is excited in parallel channels, when flow rate reduces owing to closing of a valve at common inlet of the parallel channels. If this is the case, flow regime is different between the entrance and the exit of outlet pipes connected with heating sections.

(4) Natural circulation flow rate could be predicted by the code based on a slip model within an accuracy of about 15%. This code is also applied to analysis of flow oscillation exited in low heating power region.

NOMENCLATURE

A : flow area (m^2)

a : length of pipe (m)

b : the sum of frictional loss, head, momentum difference and pressure loss at bends (Pa)

N : number of channels

P : pressure (Pa)

Re : Reynolds number (-)

w : mass velocity ($kg/m^2 \cdot s$)

$\dot{w}$: dw/dt ($kg/m^2 \cdot s^2$)

x : quality (-)

α : void fraction (-)

β : volumetric flow fraction (-)

ζ : loss coefficient (-)

λ : Darcy-Weisbach friction factor (-)

ρ : density (kg/m^3)

Subscript

b : bend

D : steam drum

d : downcomer

g : gass

i : channel

l : liquid

sp : spacer

w : water drum

REFERENCES

(1) Nakajima, I. et al., ASME 75-WA/HT-20, (1975).

(2) Fukuda, K. and Kobori, T., J. of Nuclear Science and Technology, 16, 2 (1979).

(3) Blasius, H., Mitt. Forsch Geb. Ing. -Wesen, 131 (1913).

(4) Nikuradse, J., Forsh. Geb. Ing. -Wes., 356 (1932), 1.

(5) Gibson, A.H., Hydraulics, (1952), 91 Constable & Co.

(6) Richer, H., Rohrhydraulik (3 Aufl.), (1958), 172, Springer-verlag.

(7) Jones, A.B., et al., KAPL-2208, (1962).

(8) Sugawara, S. and Kobori, T., Proceedings ANS/ASME/NRC Topical on Nuclear Reactor Thermohydraulics, NUREG/CP-6014, (1980).

(9) American Nuclear Society Proposed Standard, "Decay Energy Release Rate Following Shutdown of Uranium-Fueled Thermal Reactors", ANS 5.1 Rev., (Oct. 1973).

TABLE 1 EXPERIMENTAL CONDITIONS OF THE HEAT TRANSFER LOOP AND THE DESIGN DATA OF THE ATR DEMONSTRATION PLANT

	ITEM	HTL	FUGEN	DEM. PLANT
(1)	NUMBER OF FUEL RODS	28, 36	28	36
(2)	CHANNEL POWER (MW)	0 – 2	0 – 2.5	0 – 3.0
(3)	SHAPE OF HEATING	FLAT	–	–
			INLET PEAK	INLET PEAK
		CHOPPED COSINE	CHOPPED COSINE	CHOPPED COSINE
(4)	AXIAL PEAKING	1.35	1.35	1.3
(5)	LOCAL POWER	1.17/0.82/0.7	1.17/0.82/0.7	1.2/0.84/0.72
	DISTRIBUTION	1.11/1.01/0.65	1.0/1.0/1.0	1.11/1.01/0.65
(6)	CHANNEL FLOW RATE (ℓ/min)	0 – 330	760	820
(7)	INLET SUBCOOLING (℃)	10 – 45	≒10	≒10
(8)	STEAM DRUM PRESSURE (MPa)	0.2 – 7	6.9	7.0
(9)	INLET PIPE LENGTH (m)	10.6 (4B)	21 (2B)	16 (2B)
(10)	OUTLET PIPE LENGTH (m)	8.46 (5B)	≒16 (3B)	≒21 (3B)
		25.2, 29.1 (3B)		

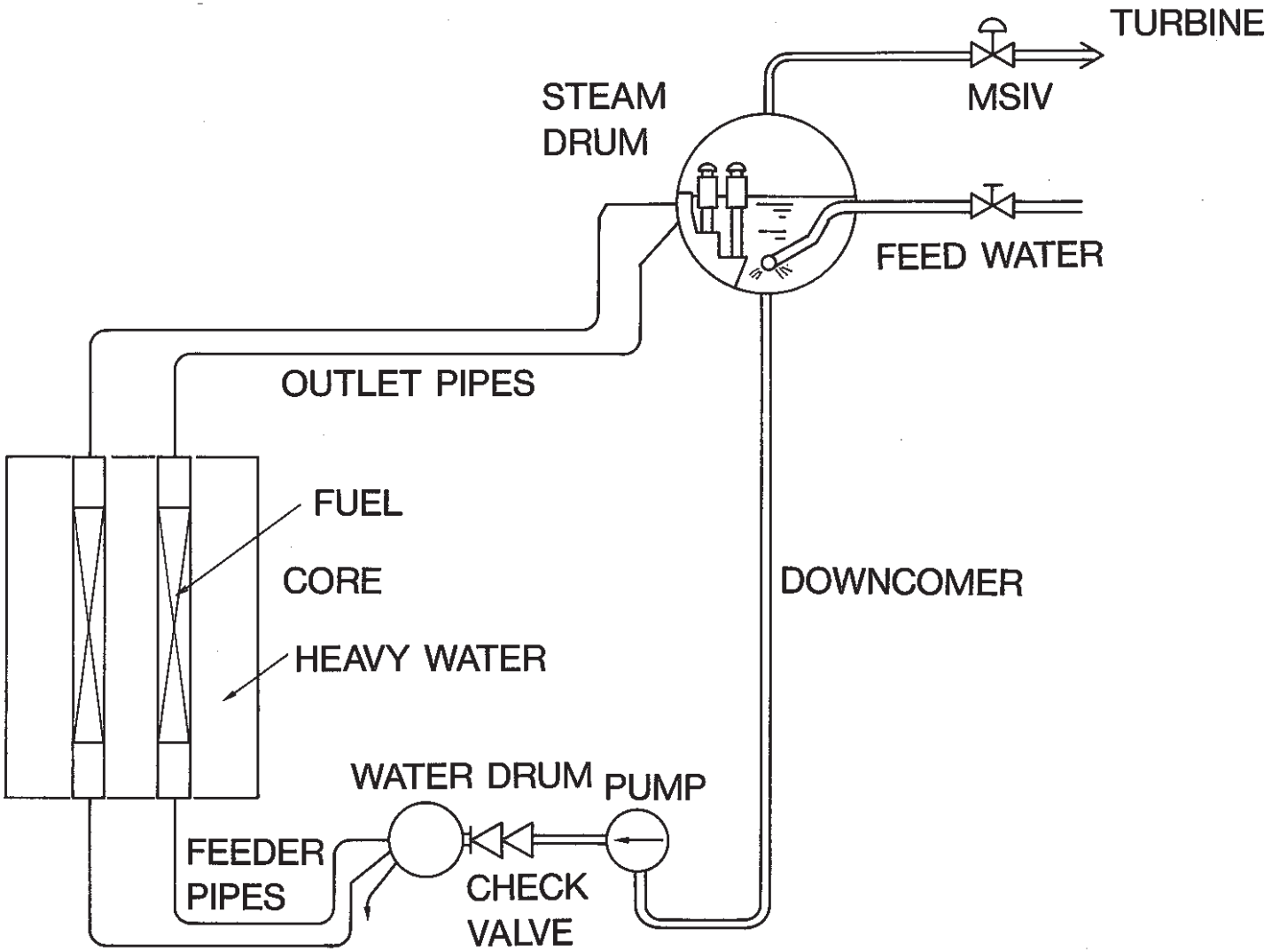

FIG.1 SCHEMATIC DIAGRAM OF ATR

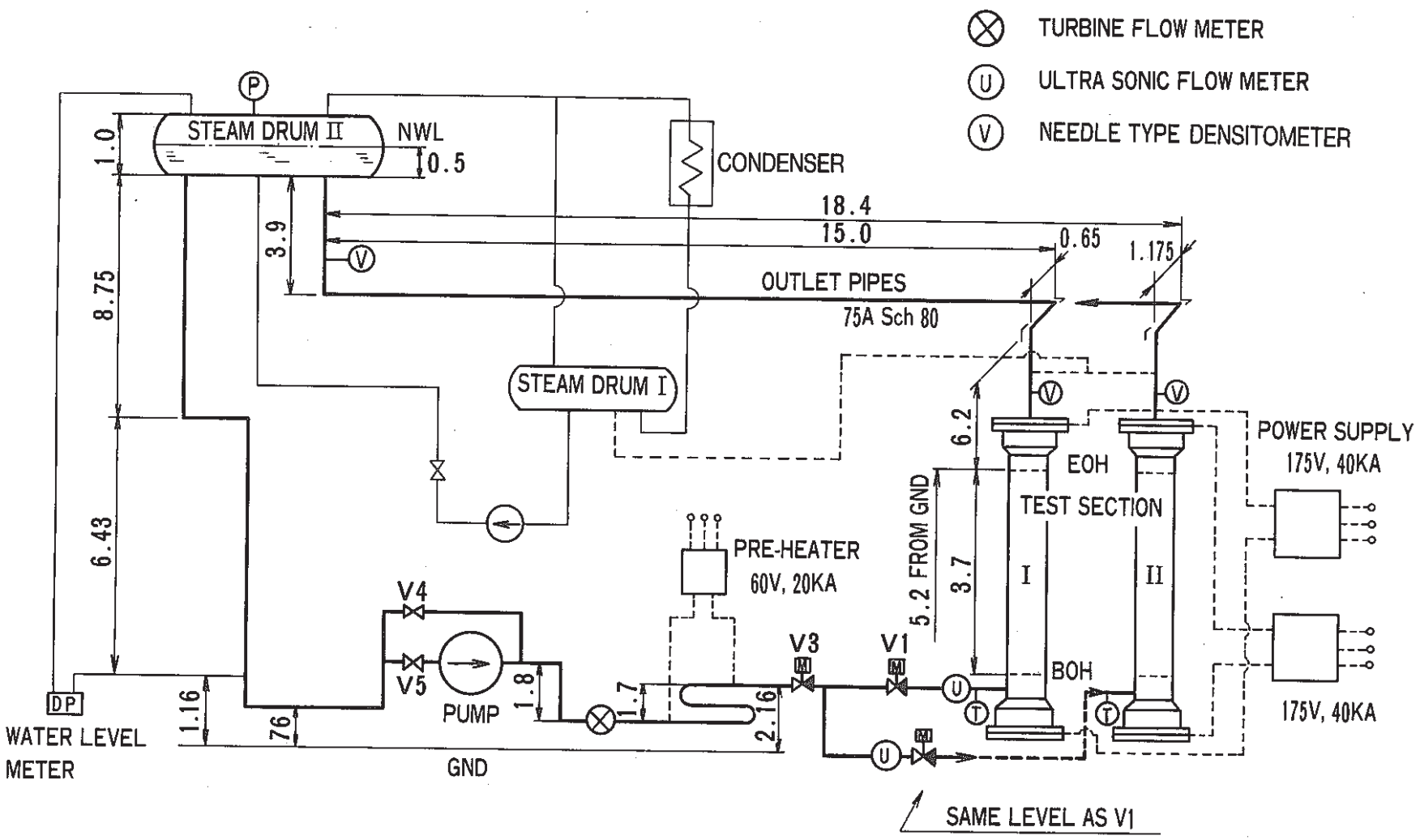

FIG. 2 FLOW DIAGRAM OF THE HEAT TRANSFER LOOP

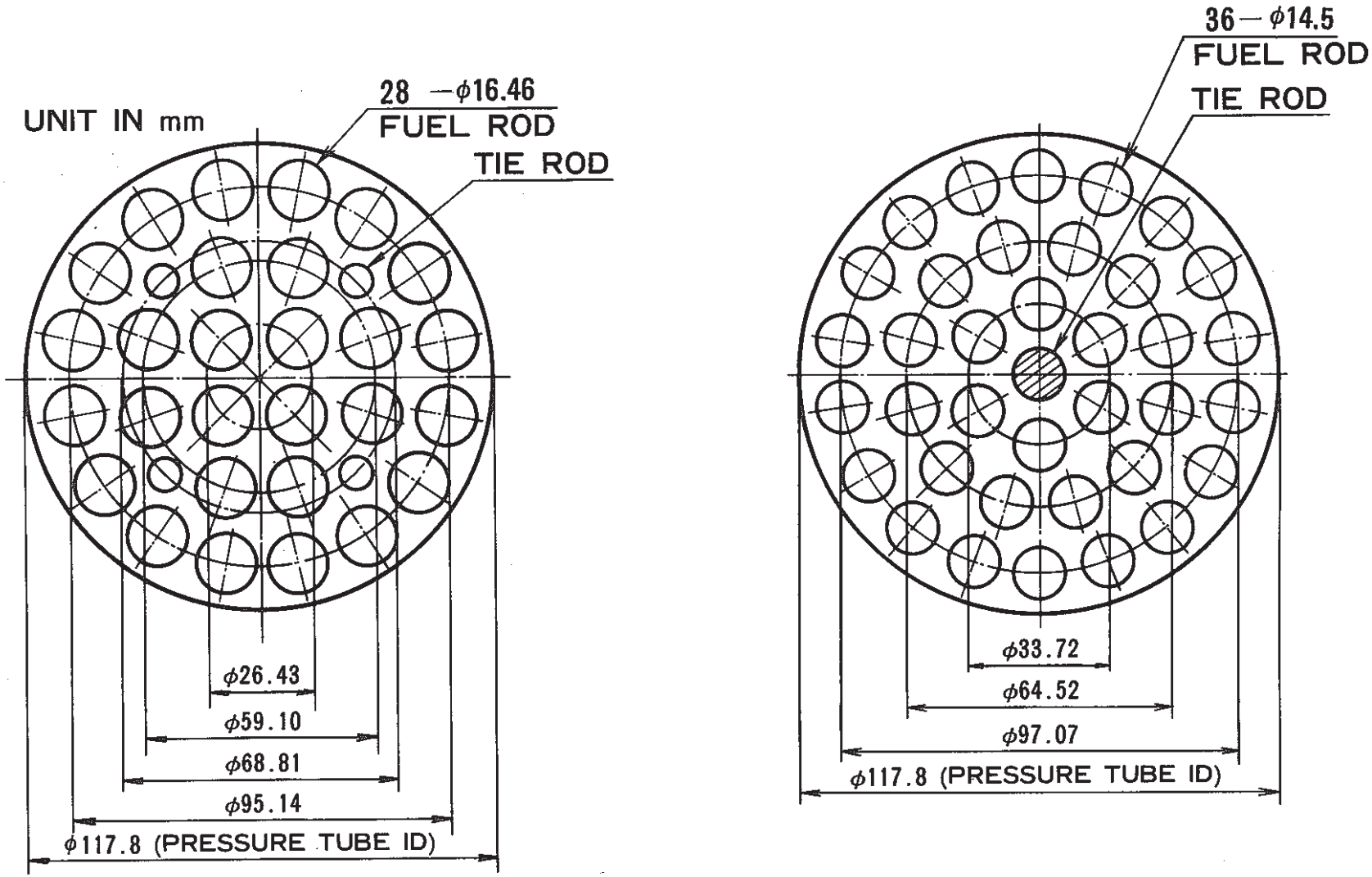

FIG. 3 CROSS SECTIONAL VIEW OF ROD BUNDLES

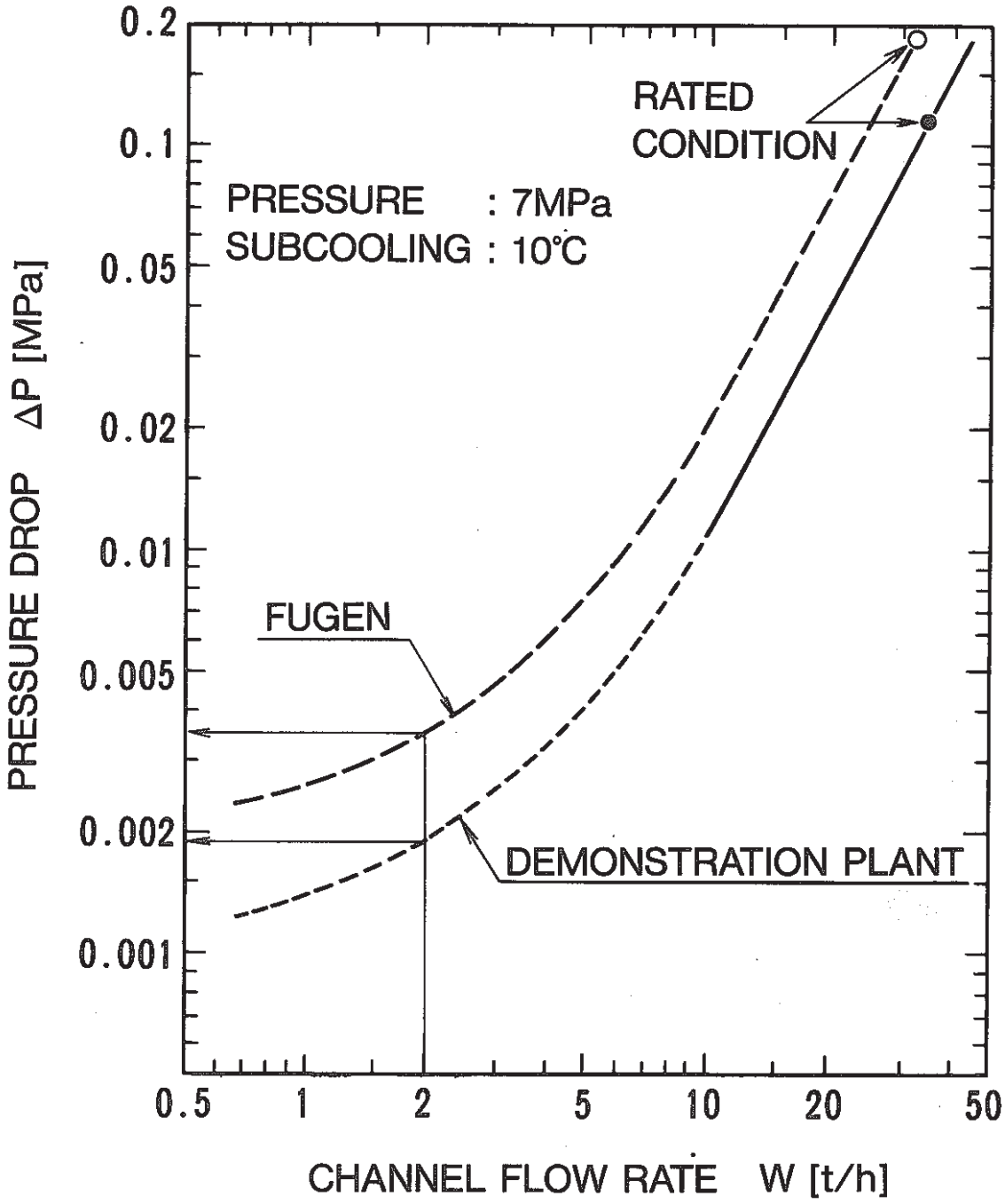

FIG.4 PRESSURE DROP BETWEEN WATER DRUM AND STEAM DRUM

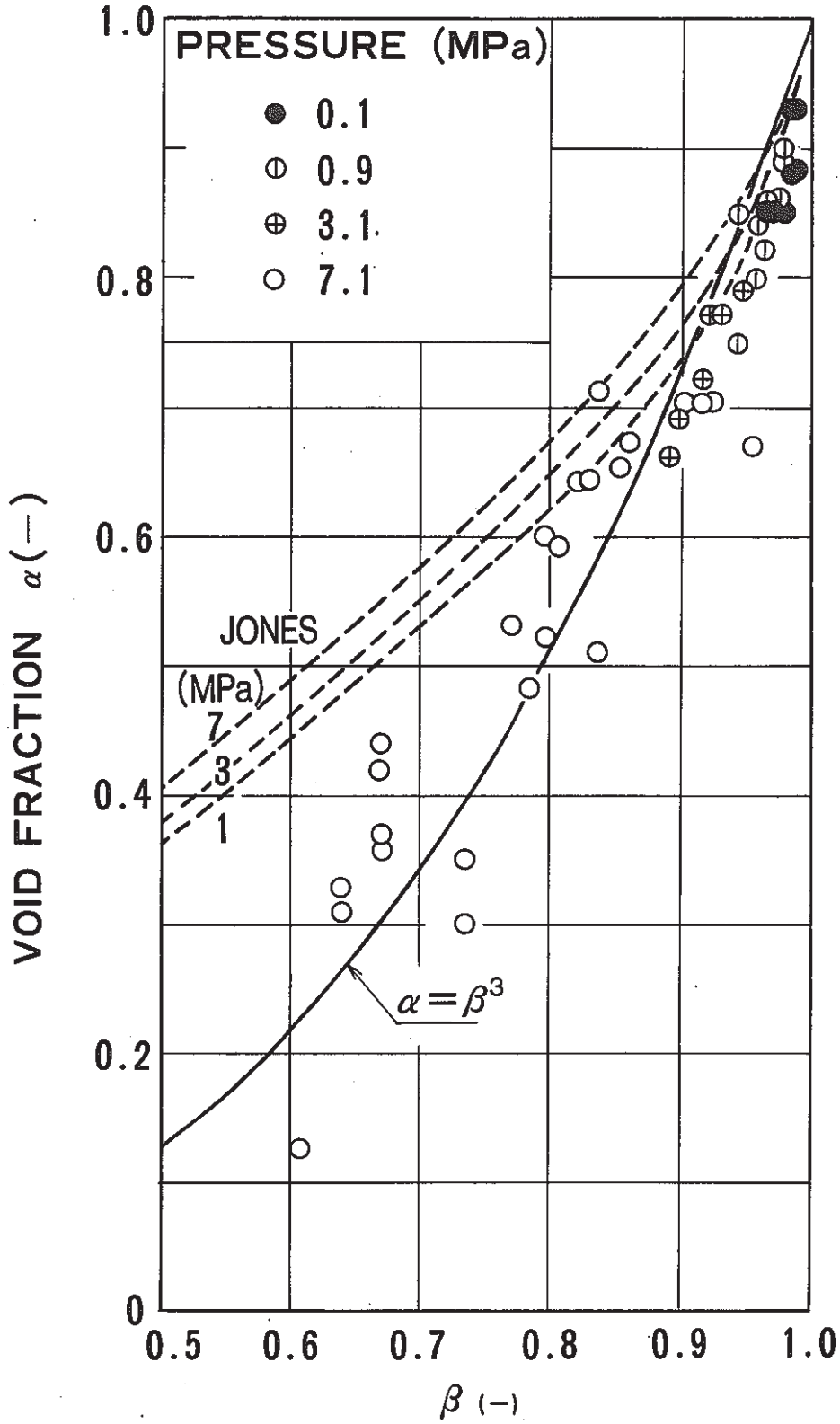

FIG.5 RELATION BETWEEN VOID FRACTION AND β

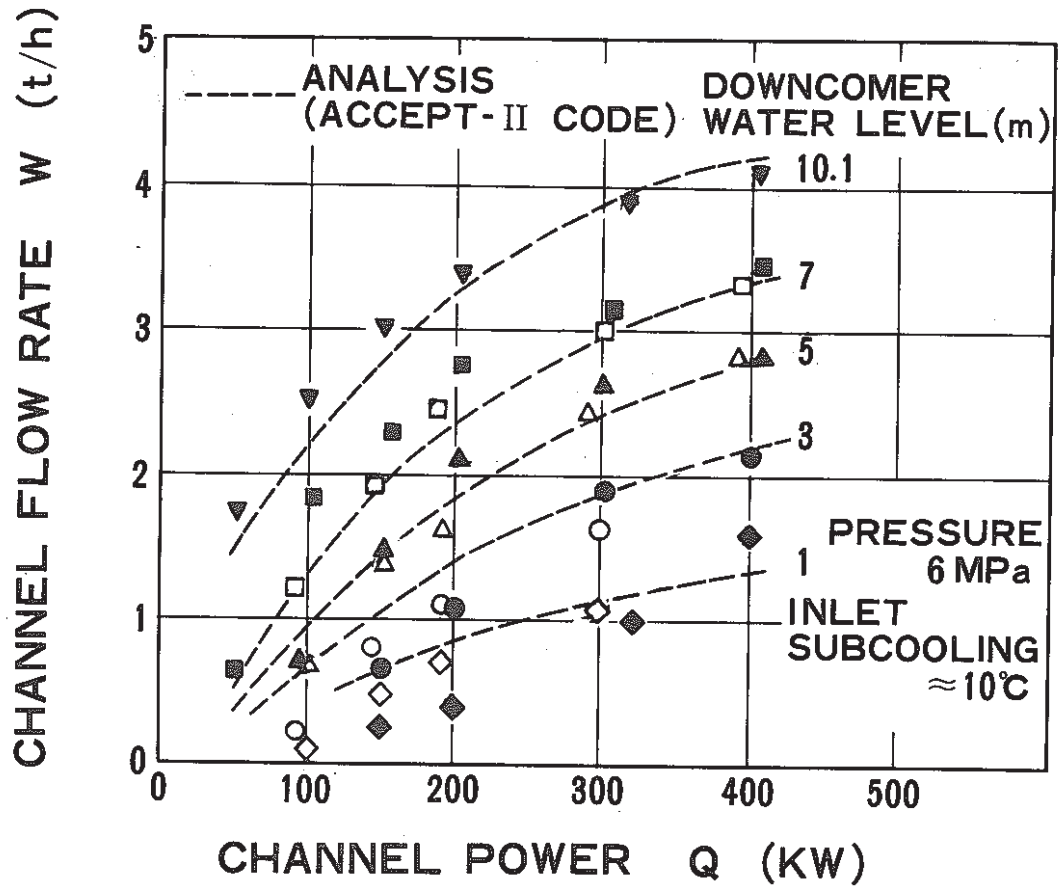

FIG.6 CHANNEL FLOW RATE VS CHANNEL POWER IN THE NATURAL CIRCULATION TEST

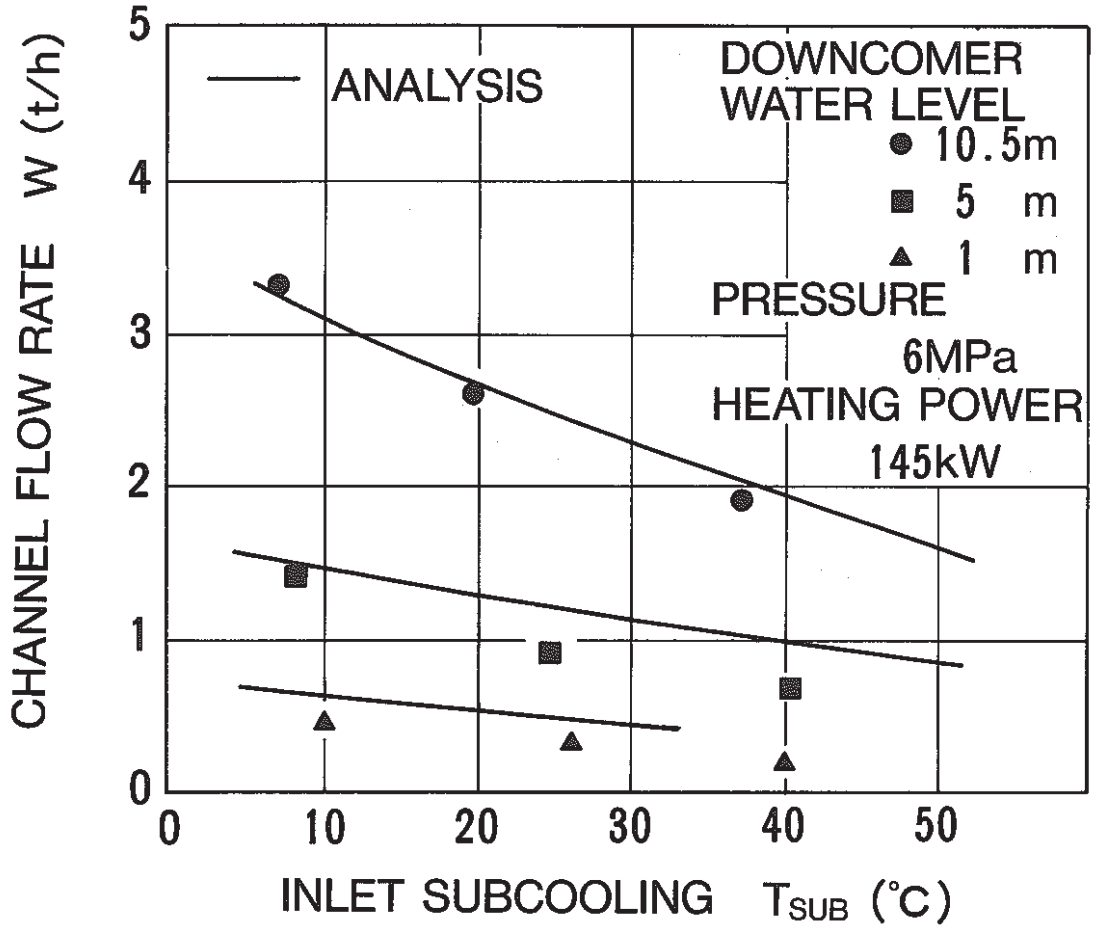

FIG.7 EFFECT OF INLET SUBCOOLING ON FLOW RATE

HEATING POWER : $50 \leqq Q \leqq 400$ (KW)
INLET SUBCOOLING : $4 \leqq T_{sub} \leqq 40$ (℃)
WATER LEVEL : $3 \leqq H \leqq 10.5$ (m)

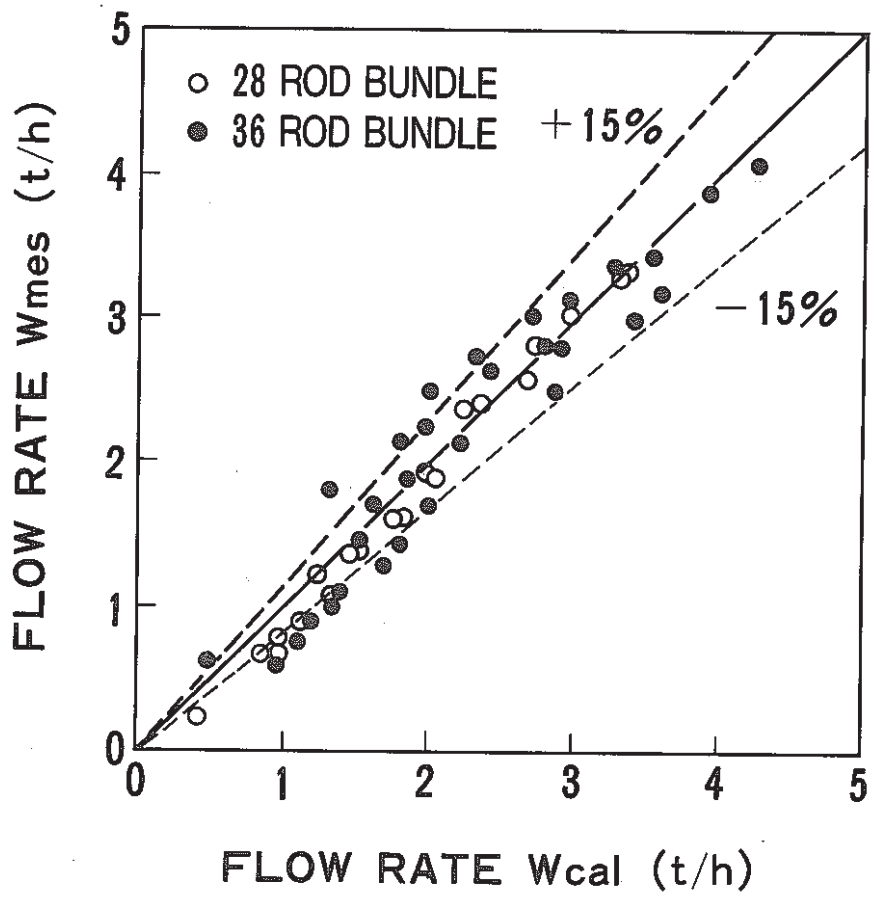

FIG.8
MEASURED FLOW RATE VS CALCULATED FLOW RATE IN NATURAL CIRCULATION

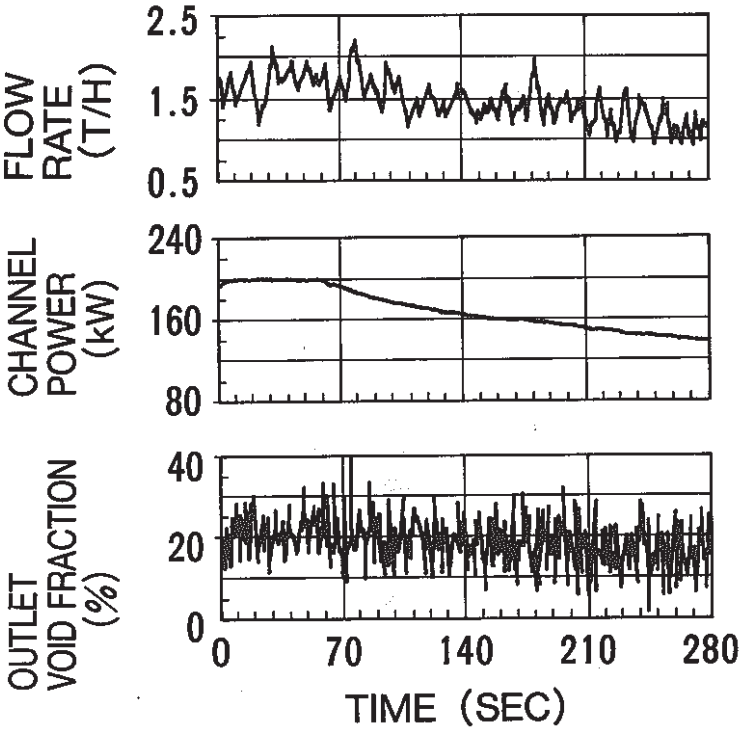

FIG.9 TIME HISTORY OF HEATING POWER TRANSIENT

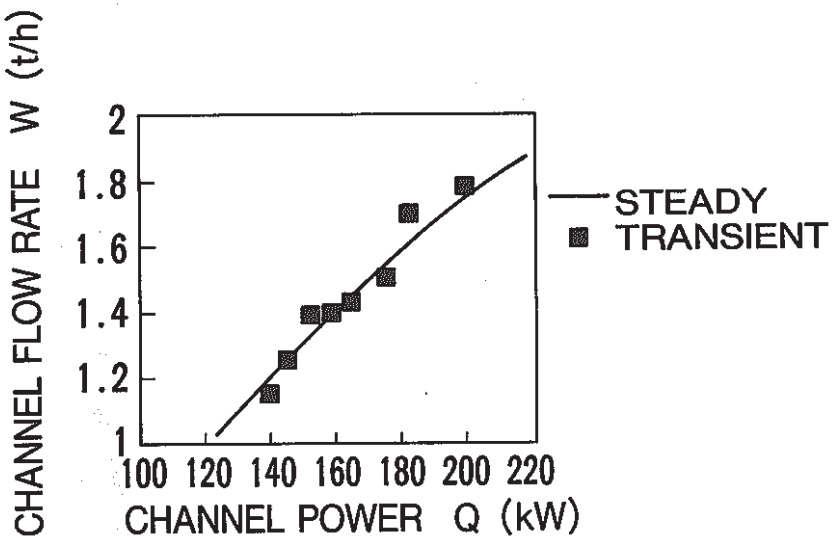

FIG.10 COMPARISON OF FLOW RATE BETWEEN STEADY STATE AND TRANSIENT

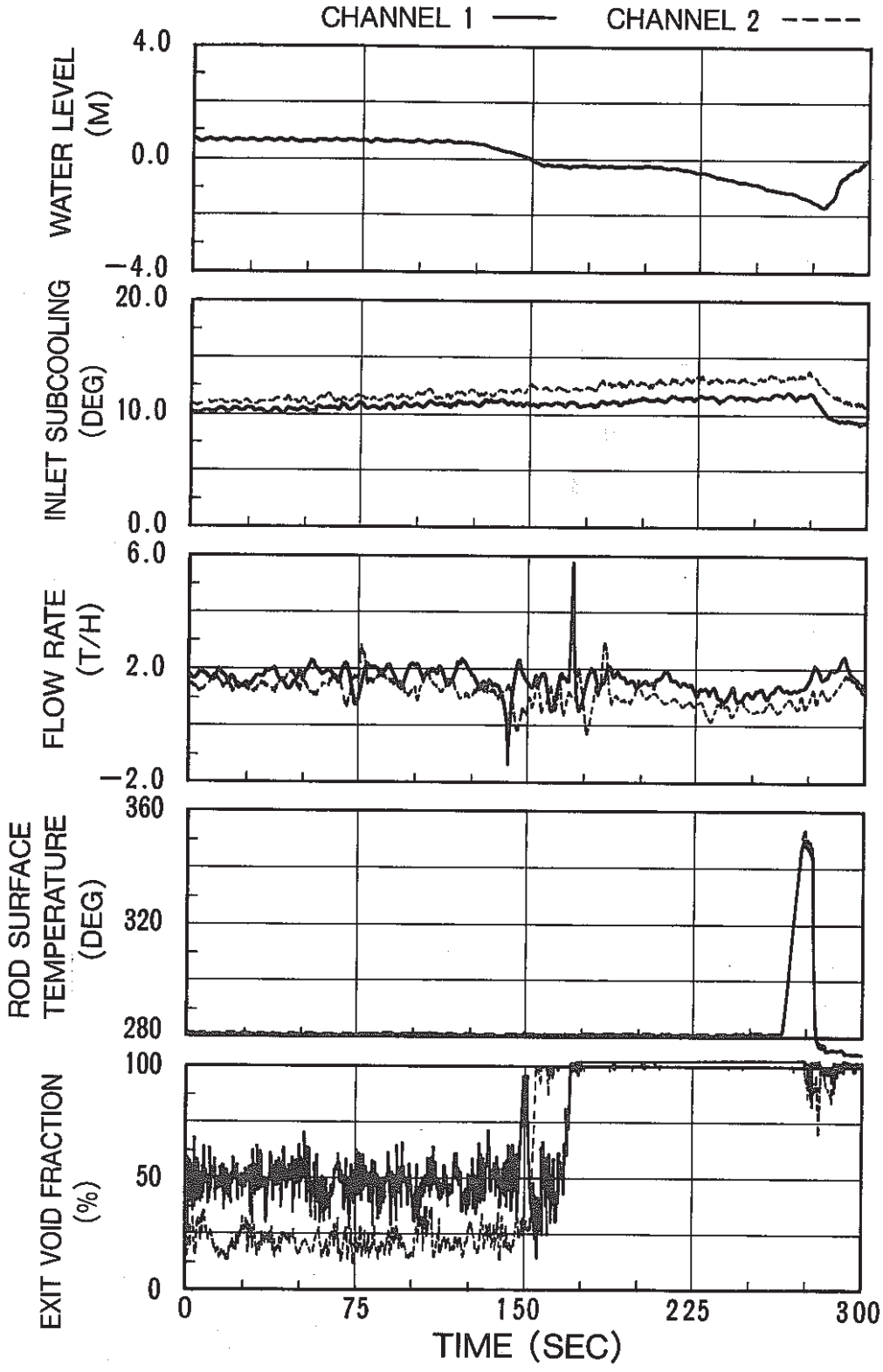

FIG.11 DRYOUT DUE TO LOWERING WATER LEVEL

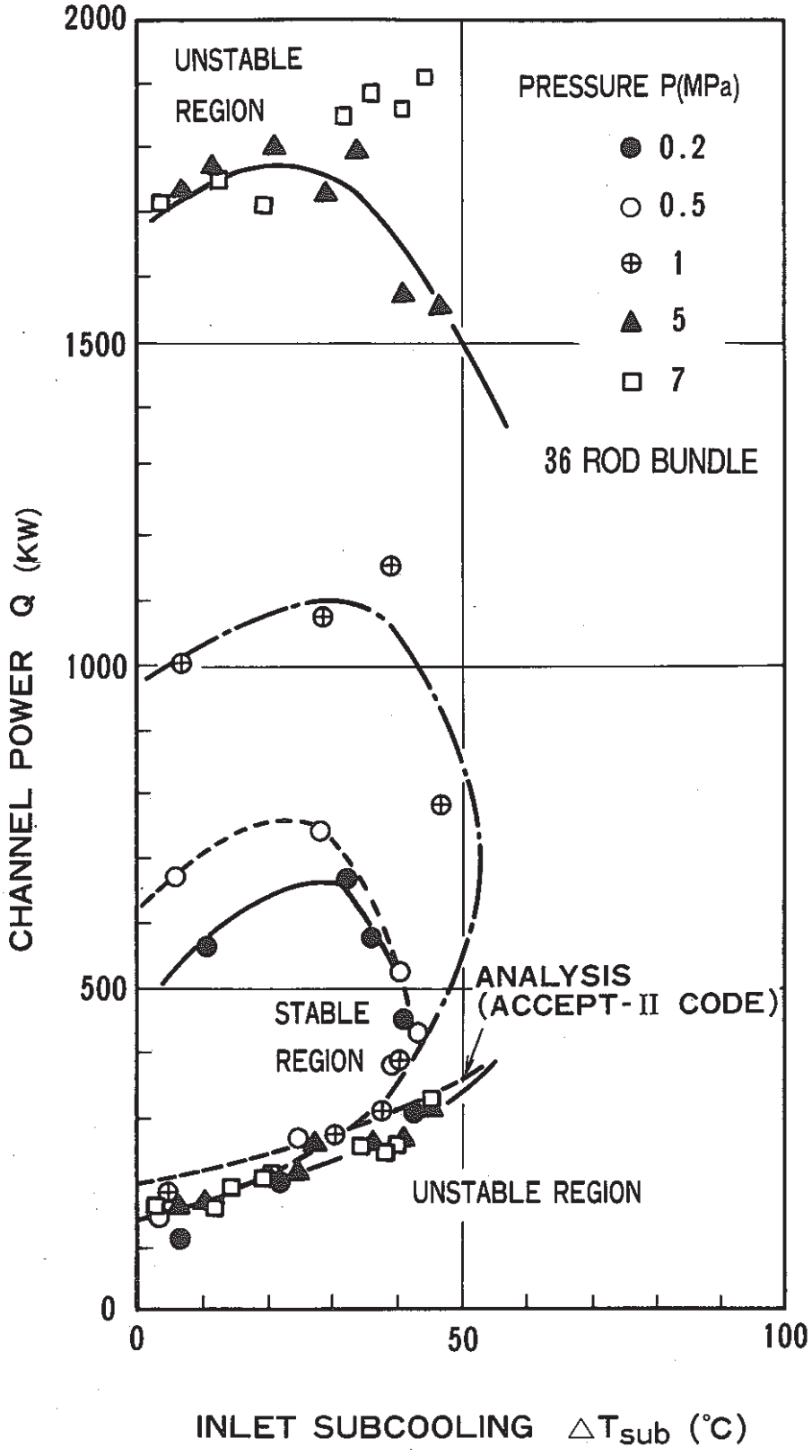

FIG. 12 STABILITY MAP OF NATURAL CIRCULATION

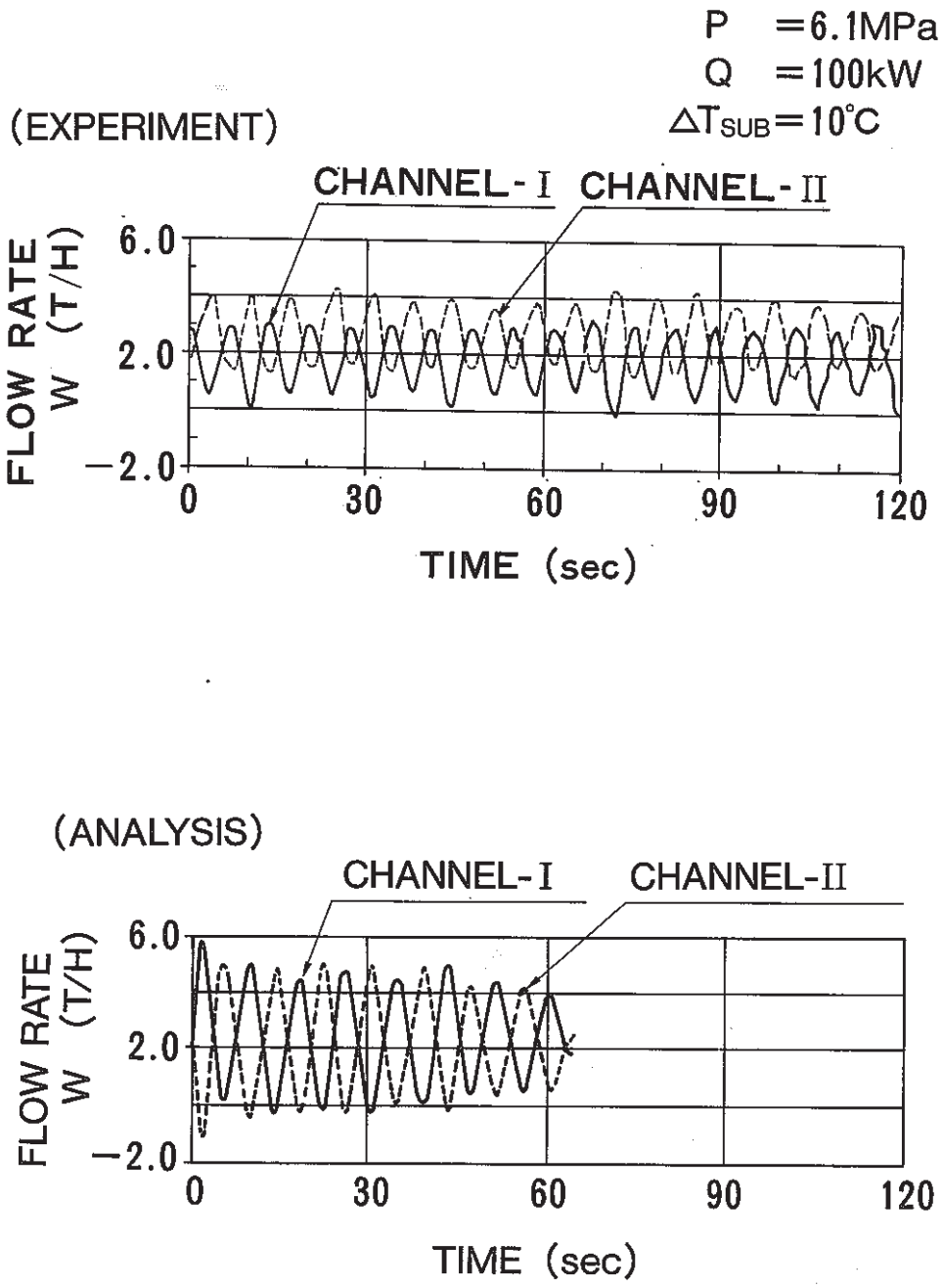

FIG.13 FLOW OSCILLATION IN LOW POWER CONDITION

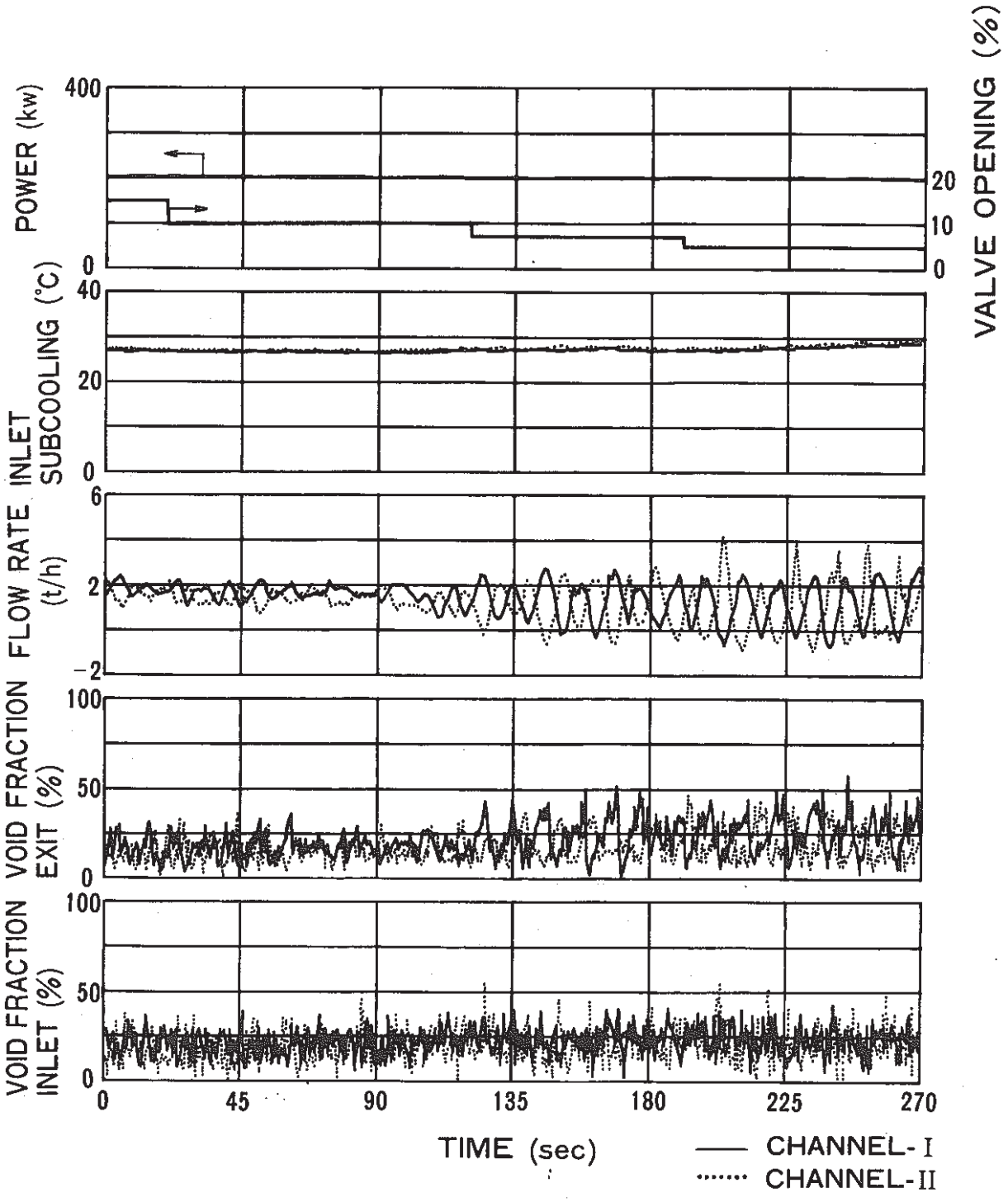

FIG.14 TIME HISTORY OF THE OSCILLATION

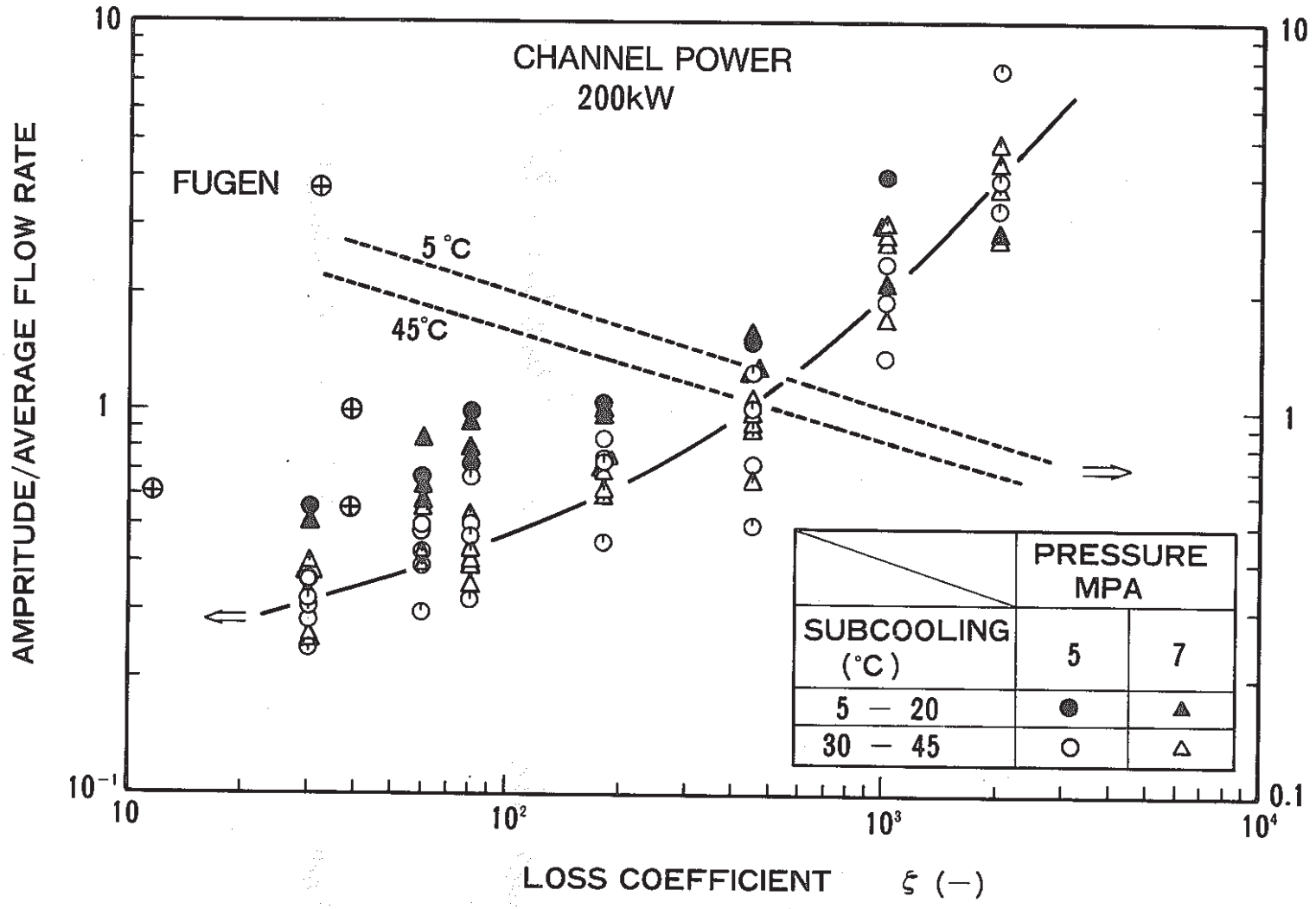

FIG. 15 RELATIONSHIP BETWEEN AMPLITUDE OF FLOW RATE AND LOSS COEFFICIENT OF COMMON VALVE